Detection and Mitigation of Reference Receiver Faults in Differential Carrier Phase Navigation Systems

Samer Khanafseh and Boris Pervan
Illinois Institute of Technology, Chicago, IL

ABSTRACT

In this paper, a methodology is developed to evaluate differential carrier phase navigation architectures subject to reference receiver faults. Carrier phase measurements can be used to provide high accuracy estimates of a user's position. But in applications that involve safety-of-life, such as in precision approach for autonomous shipboard landing, integrity also plays a critical role. One source of integrity risk is the potential for GPS reference receiver failure. Integrity risk in these situations is typically mitigated by equipping the reference station with redundant receivers. However, various approaches to utilize redundant carrier phase measurements from multiple reference receivers are possible. In this paper, we describe two new methods: an *averaging approach* where different position solutions are averaged in the position domain, and *coupled estimation approach* where the measurements from all reference receivers are coupled in the range domain and used to estimate a unified position solution. Furthermore, we investigate the impact of using these methods on accuracy and integrity from several perspectives, including availability performance, cycle resolution capabilities, implementation complexity and computational efficiency.

I. INTRODUCTION

Carrier phase measurements can be used to provide high accuracy estimates of a user's position. For life-critical GNSS applications, such as civil aircraft approach with a Ground Based Augmentation System (GBAS), extremely high levels of integrity are required. For example, for a Category I system, a maximum integrity risk of the order of 10^{-7} per aircraft approach is required with a vertical position alert limit of 10 m. However, the accuracy requirements for the GBAS application (vertical 95% accuracy on the order of 2 m) are not stringent enough to require the use of high precision carrier phase navigation [1]. As a result, these applications are usually based on snapshot positioning by computing position fixes using carrier-smoothed code. With the emergence of new aviation applications such as autonomous airborne refueling [2], [3] and autonomous shipboard landing [4], [5] and [6], where the life of pilots is involved, the vehicles are highly dynamic and complete autonomy is needed, high levels of both integrity and accuracy are required simultaneously. In these situations, the use of carrier phase measurements becomes necessary. Also, in order to achieve centimeter-level positioning accuracy using carrier phase measurements, the resolution of cycle ambiguities is required.

The integrity of the navigation system is at risk when a reference receiver fails. For the purpose of this work, a receiver fault is defined as an event on which a receiver produces anomalous measurements from either single or multiple channels. These scenarios are usually handled by equipping the reference station with multiple receivers, which provide redundancy for estimation and a means for reference receiver fault mitigation. Although multiple reference receivers are usually used for integrity, it is possible to utilize these redundant measurements to enhance accuracy as well. The improvement in accuracy that is achievable depends heavily on how these measurements are combined. In this work we develop two different approaches to process the redundant measurements from the reference receivers. The first method is a position domain weighted average position solution, where each track estimates a position, and then the individual solutions are averaged to provide one solution. (The word 'track' in this work is used to refer to a single solution obtained using one reference receiver.) The second one is the range domain coupled estimation approach. In this method, the measurements from all reference receivers are coupled with airborne measurements in the range domain and used to estimate a unified solution.

Although multiple reference receivers can be used to improve the system accuracy, the main purpose for

Accepted for publication in the IEEE Transaction on Aerospace and Electronic Systems, Feb. 2010.
This draft is not for general distribution.

installing multiple reference receivers in the reference station is for integrity. Overall, the integrity risk of the navigation system must comply with the integrity requirement under the fault-free hypothesis (H0), the single-receiver-failure hypothesis (H1) and all other failure hypotheses (H2). The H0 and H1 hypotheses are the main focus of this paper, and therefore all other failure hypotheses (multi-receiver failures, signal in space failures, etc.) will not be discussed. Although the literature provides solutions for the integrity under the H1 hypothesis for snapshot navigation systems (such as GBAS) [1], [7] and [8], H1 integrity monitoring and analysis for carrier phase navigation algorithms has not been discussed previously. As we will show in this paper, the necessity of estimating and resolving the cycle ambiguities is the main challenge in evaluating H1 integrity for high accuracy carrier phase navigation applications.

In this paper, we will start by developing a methodology to mitigate single-receiver faults to meet H1 integrity requirements for carrier phase navigation architectures. Next, different approaches to the processing of measurements from redundant receivers are described. Finally, we investigate the impact of these approaches on accuracy and integrity (both H0 and H1) from different perspectives including availability performance, cycle resolution capabilities, complexity and computational efficiency.

II. H1 HYPOTHESIS MITIGATION ALGORITHM

The H1 hypothesis is defined as a fault associated with any one, and only one, reference receiver. A fault includes any anomalous measurement that is not immediately detected by the reference station. Therefore, the broadcast reference data are affected, which in turn, induces errors in the airborne navigation system. In this work, the reference receiver mitigation algorithm will be based on the GBAS H1 algorithm [1] [7] and [8]. However because of the differences between the navigation algorithms in the two systems, significant modifications are needed.

The GBAS navigation algorithm is a snapshot estimation system that uses smoothed pseudorange measurements and estimates the user position with respect to the reference receivers by least squares estimation process [1]. In contrast, because of the mobility of the reference station in the shipboard landing and autonomous airborne refueling applications, higher levels of accuracy are required than for similar precision approach applications at land-based airfields (GBAS for example). In addition, to ensure safety and operational usefulness, the navigation architecture must provide high levels of integrity and availability. Because of the highly stringent accuracy requirements, the navigation system in these applications is based on carrier phase differential GPS (CPDGPS) positioning. In order to benefit from the high precision of CPDGPS, the correct resolution of cycle ambiguities must be ensured. A number of methods have been used in prior work to aid in the cycle resolution. A summary of the most frequently used methods is provided in [9]. For example, satellite motion can provide the observability of the cycle ambiguities [10]. Unfortunately the rate of satellite motion is relatively slow in comparison with the time scales of the precision aviation applications in hand.

The high accuracy and integrity navigation algorithms, such as the ones for autonomous airborne refueling and autonomous shipboard landing, are complicated. More details about such algorithms can be found in [2-6], [11]. For example, they usually rely on Kalman filtering the carrier phase measurements and might use additional filtering for different measurement observables (such as ionospheric-free or geometry-free observables). In addition, to reach the desired accuracy level, cycle ambiguities are usually either completely or partially fixed subject to the integrity risk requirement. As we will see in this paper, all these complexities in the fault-free navigation algorithm present tremendous challenges, compared to existing GBAS solution, in the H1 mitigation for the navigation algorithm.

Since receiver faults have a direct impact on the measurements coming out of the receivers, it might be intuitive to design a monitor to detect faults directly to the measurement level. Examples of such monitors include, Receiver Autonomous Integrity Monitor (RAIM) [12] and [13], which can be implemented on the aircraft or a B-Value monitor [8], which can be implemented on the reference station. Typically these monitors use a threshold to detect the failure that is derived based on the type of monitor, measurement error characteristics and system continuity requirements (i.e., probability of false alarm). In principle, such a monitor will pass erroneous measurements that are smaller than the derived threshold to the airborne system without taking into account the aftereffect of such anomalous measurement on the airborne position estimate. Usually, such impact is analyzed by running a separate analysis to determine if the system still meets the requirements in the presence of reference measurements anomalies. For airborne processes that include filtering and cycle resolution, this requires defining the receiver fault threat space – a task that requires rigorous effort. Since different receivers might fail differently in regards of the magnitude and shape of the fault, even under the assumption that all kinds of faults have been considered for one receiver, the threat space analysis might only apply to that specific kind of receiver. In addition, the complex airborne architecture might include a rounding process for cycle ambiguity resolution. Unlike most linear filtering

processes that are used in the airborne navigation architecture, the rounding operation is nonlinear. Therefore, performing offline analysis to determine the effectiveness of the monitor is not possible using traditional covariance analysis. The alternative is to use a Monte-Carlo simulation, which due to the span of the potential threat space and sensitivity of the resulting position error to satellite geometry, is a highly impractical method to prove compliance with tight integrity requirements of 10^{-7} for example. Instead, reference receiver failures are best detected in the position domain at the aircraft. Since the reference station has no access to the airborne measurements, airborne filtering durations, or how many ambiguities have been fixed (if partial fixing is used), it is essentially impossible for the reference station to predict the effect of an undetected reference receiver fault on the aircraft position estimate. As a result, the airborne system ultimately must be responsible for mitigating the position domain impact of reference receiver faults.

In fault detection algorithms, it is a common practice to compute a test statistic and compare it to a predefined threshold. In receiver failure detection, as we will see shortly, the vertical protection level (*VPL*) and the vertical alert limit (*VAL*) mimic the test statistics and the threshold, respectively. VAL is a vertical containment limit requirement representing the maximum tolerable vertical position error. VPL is defined as a statistical overbound of the vertical position errors and is derived from the associated integrity risk allocation. Throughout the derivations in this work, the vertical component of the position error is used exclusively because it is usually the most stringent for precision aviation applications. However, if needed, the horizontal or lateral components can be treated similarly. In this context, the probability of hazardously misleading vertical information $P_v(MI)$ (equivalent to the integrity risk) is defined as the probability that the vertical position error exceeds VAL due to H0 and H1 hypotheses only. H2 hypothesis (events not covered by H0 or H1 such as ranging source faults and simultaneous multiple reference receiver faults) are allocated a separate budget, $P(H_2)$, from the total integrity risk. Since the H0 and H1 hypotheses are mutually exclusive and exhaustive events and assuming the reference station is equipped with *M* receivers (each is possible to fail), $P_v(MI)$ can be written as,

$$P_v(MI) = P_v(MI \mid H_0)\, P(H_0) + \sum_{j=1}^{M} P_v(MI \mid H_{1j})\, P(H_{1j}) \qquad (1)$$

where,

$$P(H_{1j}) = P(H_1)/M$$

$$P(H_0) = 1 - M\, P(H_{1j}) - P(H_2) \approx 1$$

In this work we equally distribute the allocation of $P_v(MI)$ on H0 and all H1j hypotheses. Therefore, each hypothesis will have an equal integrity risk budget of $P_v(MI)/(M+1)$. Using this quantity ($P_v(MI)/(M+1)$) in Equation 1, $P_v(MI \mid H_0)$ and $P_v(MI \mid H_{1j})$ become

$$P_v(MI \mid H_0) = \frac{P_v(MI)}{(M+1)\,P(H_0)} \cong \frac{P_v(MI)}{(M+1)} \qquad (2)$$

$$P_v(MI \mid H_{1j}) = \frac{M\, P_v(MI)}{(M+1)P(H_1)} \qquad (3)$$

Using Equations 2 and 3, a corresponding value of VPL_{H0} and VPL_{H1j} is computed, the latter corresponding to the hypothesis of a failure in the j^{th} receiver. From $P_v(MI|H_0)$, a probability coefficient K_{ffmd} is computed to establish VPL_{H0},

$$VPL_{H0} = K_{ffmd}\, \sigma_{v|H0} \qquad (4)$$

where,

K_{ffmd} is the fault-free missed detection multiplier and is computed from the inverse of the standard normal distribution cumulative distribution function (Φ) as

$$K_{ffmd} = -\Phi^{-1}\left(\frac{P_v(MI \mid H_0)}{2}\right) = -\sqrt{2}\,\mathrm{erf}^{-1}\left(P_v(MI \mid H_0) - 1\right)$$

$\sigma_{v|H0}$: is the standard deviation of the vertical estimate error under the H0 hypothesis (all reference receivers are used). The details of how $\sigma_{v|H0}$ is generated will be discussed in the next section.

From $P(MI|H_{1j})$, K_{md} is computed, in a similar way to K_{ffmd}, to establish VPL_{H1j}. However, VPL_{H1j} represents a statistical overbound on the vertical position estimate error under the hypothesis that receiver *j* has failed. As a result, if the failed measurement from the j^{th} receiver is used, it will induce an error (bias) in the vertical component of the position estimate ($\hat{v}_0$) (under the H0 hypothesis). Notice, however, that the vertical position estimate excluding the j^{th} receiver (under the H1j hypothesis) will be the best estimate of the fault-free vertical component ($\hat{v}_{1j}$) of the relative position vector. Therefore, for VPL_{H1j}, the best estimate of the vertical component of the failure magnitude (bias) in the position domain is $\left|\hat{v}_0 - \hat{v}_{1j}\right|$, which is used to compute VPL_{H1j} as,

$$VPL_{H1j} = \left|\hat{v}_0 - \hat{v}_{1j}\right| + K_{md}\, \sigma_{v|H1j} \qquad (5)$$

where $\sigma_{v|H1j}$ is the standard deviation of the vertical estimate error under the H1j hypothesis (using all reference receivers except the j^{th} receiver). Detailed derivations of Equations 4 and 5 are provided in Appendix A. As with $\sigma_{v|H0}$ above, we will describe how to compute this standard deviation shortly. Because at any instant we do not know which hypothesis is true and because of the conservative equal allocation on all hypotheses, *VPL* is the computed as the maximum value of all protection limits (Equation 6).

$$VPL_{H1} = \max_{j=1:M} \left\{ VPL_{H0}, VPL_{H1j} \right\} \tag{6}$$

Notice that, in order to compute VPL_{H1j}, it is necessary to have access to the relative position estimates ($\hat{v}_0$ and $\hat{v}_{1j}$), which are necessary to compute $\left|\hat{v}_0 - \hat{v}_{1j}\right|$. Therefore, the calculation of VPL_{H1j} requires access to the measurements and needs to be executed epoch by epoch.

If continuity requirements exist, further attention must be paid to the detection false alarm rate. (Continuity risk is the probability of a detected but unscheduled navigation function interruption after an operation has been initiated.) Since both $\hat{v}_0$ and $\hat{v}_{1j}$ are estimated subject to measurement noise, they are both random. Therefore, the term $\left|\hat{v}_0 - \hat{v}_{1j}\right|$ in Equation 5 is random, which makes VPL_{H1j} a random variable as well. The randomness in VPL_{H1j} might cause *VPL* to exceed *VAL* even under fault-free conditions, which in turn will trigger a false alarm. The probability of false alarm due to the randomness in $\left|\hat{v}_0 - \hat{v}_{1j}\right|$ must comply with the corresponding fault free continuity risk requirement. In response, a predictive VPL_{H1j} (referred to as $PVPL_{H1j}$) is computed taking into account the randomness of $\left|\hat{v}_0 - \hat{v}_{1j}\right|$ through $\sigma_{|v0\text{-}v1j|}$ and a probability multiplier, referred to as K_{ffc}, that is based on the fault free continuity risk requirement (C_{req}) as in Equation 7.

$$PVPL_{H1j} = K_{ffc}\,\sigma_{\left|v_0 - v_{1j}\right|} + K_{md}\,\sigma_{v|H1j} \tag{7}$$

where K_{ffc} is computed as $K_{ffc} = -\sqrt{2}\,\mathrm{erf}^{-1}\left(C_{req} - 1\right)$.

Before initiating an operation (aircraft approach for example), $PVPL_{H1j}$ is computed for the whole operation. If $PVPL_{H1j}$ exceeds *VAL*, then the probability of VPL_{H1j} exceeding *VAL* due to the fault free randomness in $\left|\hat{v}_0 - \hat{v}_{1j}\right|$ exceeds the continuity risk requirement. In other words, the predicted continuity risk for the operation exceeds the continuity risk requirement and therefore the operation must not be initiated.

Although computing VPL_{H0} and VPL_{H1j} was addressed in previous work for GBAS [1], [7] and [8], it is a much more significant challenge for carrier phase navigation algorithms, which may include Kalman filtering and cycle ambiguity fixing. Before going into details of how *VPL*s are computed (i.e., the σ terms in Equations 4, 5 and 7), it must be acknowledged that the existence of redundant reference measurements presents different choices of how these measurements can be treated. In this work, two different approaches toward using reference measurements will be presented. The first is referred to as the averaging approach, where individual estimates between the user receiver and each reference receiver are combined in the position domain by a weighted average. The other approach, which is referred to as the coupled estimation approach, combines the measurements in the range domain and then estimates the relative position vector. To facilitate the development below, we use a shipboard landing example, with three shipboard receivers and a single airborne receiver, as a framework for discussion of the two methods. However, the methods themselves are generally applicable to any differential carrier phase system involving multiple receivers.

III. AVERAGING APPROACH

In the averaging method, each airborne-shipboard receiver pair is processed individually and the relative position vector for each pair is estimated. The known lever arms between the fixed antennas onboard the ship are converted to baseline vectors in the navigation frame using a variable ship attitude model. (In this work, attitude and lever arm survey errors are assumed to be negligible.) Knowing the baseline vectors between the antennas and a certain point of interest (say the touchdown point), all estimated vectors can be translated to one reference relative vector with respect to the touchdown point.

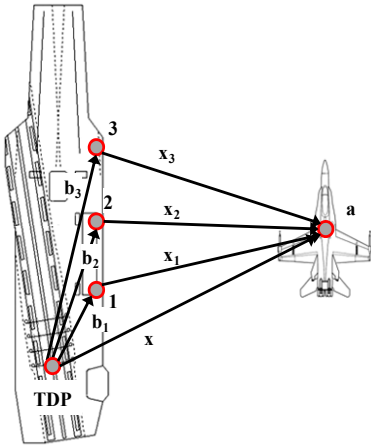

Figure 1: Schematic Diagram for a Ship Equipped with Multi Antennas/Receivers and an Aircraft with a Single Airborne Antenna/Receiver.

For example, if three antennas/receivers are used on the ship, as seen in Figure 1, three simplified double difference (user minus reference and satellite minus master-satellite) carrier phase measurement equations can be written as shown in Equations 8, 9 and 10. (Other states such as multipath and atmospheric states can also be added but are not included here for clarity in the development.)

$$\nabla\Delta\boldsymbol{\varphi}_1 = \begin{bmatrix}\Delta\mathbf{e}^T & \mathbf{I}\lambda\end{bmatrix}\begin{bmatrix}\mathbf{x}_1 \\ \nabla\Delta\mathbf{N}_1\end{bmatrix} + \boldsymbol{\varepsilon}_{\Delta\phi 1} \tag{8}$$

$$\nabla\Delta\boldsymbol{\varphi}_2 = \begin{bmatrix}\Delta\mathbf{e}^T & \mathbf{I}\lambda\end{bmatrix}\begin{bmatrix}\mathbf{x}_2 \\ \nabla\Delta\mathbf{N}_2\end{bmatrix} + \boldsymbol{\varepsilon}_{\Delta\phi 2} \tag{9}$$

$$\nabla\Delta\boldsymbol{\varphi}_3 = \begin{bmatrix}\Delta\mathbf{e}^T & \mathbf{I}\lambda\end{bmatrix}\begin{bmatrix}\mathbf{x}_3 \\ \nabla\Delta\mathbf{N}_3\end{bmatrix} + \boldsymbol{\varepsilon}_{\Delta\phi 3} \tag{10}$$

where,

$\nabla\Delta\boldsymbol{\varphi}_1$, $\nabla\Delta\boldsymbol{\varphi}_2$ and $\nabla\Delta\boldsymbol{\varphi}_3$: the double difference carrier phase measurement vectors for tracks 1, 2 and 3

$\Delta\mathbf{e}$: matrix of stacked differenced unit line of sight vectors

λ : carrier phase wavelength

$\mathbf{x}_1$, $\mathbf{x}_2$ and $\mathbf{x}_3$: relative position vector between the aircraft and reference receivers 1, 2 and 3, respectively.

$\nabla\Delta\mathbf{N}_1$, $\nabla\Delta\mathbf{N}_2$ and $\nabla\Delta\mathbf{N}_3$: double difference ambiguity vectors for tracks 1, 2 and 3

$\boldsymbol{\varepsilon}_{\Delta\phi 1}$, $\boldsymbol{\varepsilon}_{\Delta\phi 2}$ and $\boldsymbol{\varepsilon}_{\Delta\phi 3}$: the double difference carrier phase measurement noise vectors for tracks 1, 2 and 3

Each relative position vector can be estimated separately using a Kalman filter (with or without partially fixed ambiguities) and then the true relative position vector $\mathbf{x}$ between the aircraft and the touchdown point (TDP) can be written in terms of the three individually estimated vectors $\hat{\mathbf{x}}_1$, $\hat{\mathbf{x}}_2$ and $\hat{\mathbf{x}}_3$ as:

$$\mathbf{x} = \hat{\mathbf{x}}_1 + \mathbf{b}_1 + \boldsymbol{\varepsilon}_{x1} = \hat{\mathbf{x}}_2 + \mathbf{b}_2 + \boldsymbol{\varepsilon}_{x2} = \hat{\mathbf{x}}_3 + \mathbf{b}_3 + \boldsymbol{\varepsilon}_{x3} \tag{11}$$

where ε_{x1}, ε_{x2} and ε_{x3} are the estimation errors for relative position vectors $\mathbf{x}_1$, $\mathbf{x}_2$ and $\mathbf{x}_3$, respectively.

Under the H0 hypothesis, where all three antennas are assumed fault free, these three vectors can be averaged to produce one vector $\hat{\mathbf{x}}_0$ (the subscript zero is used to refer to the H0 case). $\hat{\mathbf{x}}_{1j}$, which is used in computing $\mathrm{VPL}_{\mathrm{H1}j}$ for the H1j hypothesis, is computed similarly but excluding the j^{th} relative position estimate ($\hat{\mathbf{x}}_j$). Notice that averaging, must account for the quality of and correlation between the individual estimates. Therefore, a weighted average is performed. Using Equation 11, $\hat{\mathbf{x}}_0$ can be estimated by solving the following model in a least square sense,

$$\begin{bmatrix}\hat{\mathbf{x}}_1 + \mathbf{b}_1 \\ \hat{\mathbf{x}}_2 + \mathbf{b}_2 \\ \hat{\mathbf{x}}_3 + \mathbf{b}_2\end{bmatrix} = \begin{bmatrix}\mathbf{I} \\ \mathbf{I} \\ \mathbf{I}\end{bmatrix}\mathbf{x} + \begin{bmatrix}\boldsymbol{\varepsilon}_{x1} \\ \boldsymbol{\varepsilon}_{x2} \\ \boldsymbol{\varepsilon}_{x3}\end{bmatrix} \Rightarrow \mathbf{z}_0 = \mathbf{H}_0\mathbf{x} + \mathbf{v}_0 \tag{12}$$

With the 3×3 covariance matrix $\hat{\mathbf{P}}_{xn\,xm}$ defined as $E\{\boldsymbol{\varepsilon}_{xn}\,\boldsymbol{\varepsilon}_{xm}^T\}$, the covariance matrix of the error vector $\mathbf{v}_0$ is written as,

$$\mathbf{R}_0 = E\{\mathbf{v}_0\mathbf{v}_0^T\} = \begin{bmatrix}\hat{\mathbf{P}}_{x1x1} & \hat{\mathbf{P}}_{x1x2} & \hat{\mathbf{P}}_{x1x3} \\ \hat{\mathbf{P}}_{x1x2}^T & \hat{\mathbf{P}}_{x2x2} & \hat{\mathbf{P}}_{x2x3} \\ \hat{\mathbf{P}}_{x1x3}^T & \hat{\mathbf{P}}_{x2x3}^T & \hat{\mathbf{P}}_{x3x3}\end{bmatrix} \tag{13}$$

Since the aircraft measurement is common to all three baselines and is used in estimating the three position estimates $\hat{\mathbf{x}}_1$, $\hat{\mathbf{x}}_2$ and $\hat{\mathbf{x}}_3$, the off diagonal blocks of $\mathbf{R}_0$ ($\hat{\mathbf{P}}_{x1x2}$, $\hat{\mathbf{P}}_{x1x3}$ and $\hat{\mathbf{P}}_{x2x3}$) are not zero and must be evaluated. In GBAS, the off diagonal terms could easily be expressed in terms of raw measurement noise standard deviations because the position estimation in GBAS is based on a least squares snapshot positioning. In navigation algorithms that are under consideration in this work, Kalman filters are usually used to estimate the individual relative vectors. Therefore, it is quite challenging to write the off diagonal block matrices in $\mathbf{R}_0$ in terms of the raw measurement noise variance. A new method to account for correlated KF estimates must be derived.

Correlated Kalman Filters

In this subsection, the cross covariance of two correlated state vectors that were each estimated using Kalman filters is derived. To be general, no assumption is made in this derivation about what kind of states these vectors include (i.e., they might include position, ambiguities, multipath or atmospheric states). These two estimated vectors will be referred to as $\hat{\mathbf{y}}_1$ and $\hat{\mathbf{y}}_2$. The measurement update will be discussed first. In order to estimate $\mathbf{y}_1$ and $\mathbf{y}_2$ at time k, the Kalman filter equations 14 and 15 are used, respectively [14]. (Notice that the time subscript k is not used in these equations for clarity.)

$$\hat{\mathbf{y}}_1 = \bar{\mathbf{y}}_1 + \mathbf{K}_1\left(\mathbf{z}_1 - \mathbf{H}_1\bar{\mathbf{y}}_1\right) \tag{14}$$

$$\hat{\mathbf{y}}_2 = \bar{\mathbf{y}}_2 + \mathbf{K}_2\left(\mathbf{z}_2 - \mathbf{H}_2\bar{\mathbf{y}}_2\right) \tag{15}$$

where,

$\bar{\mathbf{y}}_1$ and $\bar{\mathbf{y}}_2$: *a priori* estimates of state vectors $\mathbf{y}_1$ and $\mathbf{y}_2$

$\mathbf{K}_1$ and $\mathbf{K}_2$: Kalman gains for $\mathbf{y}_1$ and $\mathbf{y}_2$

$\mathbf{z}_1$ and $\mathbf{z}_2$: measurements from receivers 1 and 2

$\mathbf{H}_1$ and $\mathbf{H}_2$: the observation matrices for $\mathbf{y}_1$ and $\mathbf{y}_2$

The measurement models for $\mathbf{y}_1$ and $\mathbf{y}_2$ can be defined as

$$\mathbf{z}_1 = \mathbf{H}_1 \mathbf{y}_1 + \mathbf{v}_1 \quad (16)$$

$$\mathbf{z}_2 = \mathbf{H}_2 \mathbf{y}_2 + \mathbf{v}_2 \quad (17)$$

Therefore, by definition, the post measurement cross covariance matrix ($\hat{\mathbf{P}}_{y1y2}$) between the error in the estimates $\hat{\mathbf{y}}_1$ and $\hat{\mathbf{y}}_2$ is,

$$\hat{\mathbf{P}}_{yx1y2} = E\left\{\left(\mathbf{y}_1 - \hat{\mathbf{y}}_1\right)\left(\mathbf{y}_2 - \hat{\mathbf{y}}_2\right)^T\right\} \quad (18)$$

Substituting Equations 14, 15, 16 and 17 in to 18, $\hat{\mathbf{P}}_{y1y2}$ becomes,

$$\begin{aligned}\hat{\mathbf{P}}_{y1y2} = E\{&\left[\left(\mathbf{I} - \mathbf{K}_1\mathbf{H}_1\right)\left(\mathbf{y}_1 - \overline{\mathbf{y}}_1\right) - \mathbf{K}_1\mathbf{v}_1\right] \\ &\left[\left(\mathbf{I} - \mathbf{K}_2\mathbf{H}_2\right)\left(\mathbf{y}_2 - \overline{\mathbf{y}}_2\right) - \mathbf{K}_2\mathbf{v}_2\right]^T\}\end{aligned} \quad (19)$$

where $\mathbf{v}_1$ and $\mathbf{v}_2$ are the measurement noise vectors for $\mathbf{z}_1$ and $\mathbf{z}_2$, respectively. Assuming that the prior estimates and the current measurement noises are independent, Equation 19 can be simplified to

$$\begin{aligned}\hat{\mathbf{P}}_{y1y2} = &\left(\mathbf{I} - \mathbf{K}_1\mathbf{H}_1\right)E\left\{\left(\mathbf{y}_1 - \overline{\mathbf{y}}_1\right)\left(\mathbf{y}_2 - \overline{\mathbf{y}}_2\right)^T\right\}\left(\mathbf{I} - \mathbf{K}_2\mathbf{H}_2\right)^T \\ &+ \mathbf{K}_1 E\left\{\mathbf{v}_1\,\mathbf{v}_2^T\right\}\mathbf{K}_2^T\end{aligned} \quad (20)$$

The expected value in the first term in the right hand side will be referred to as $\overline{\mathbf{P}}_{y1y2}$ (pre-measurement cross covariance matrix) and will be discussed shortly in the time propagation of the Kalman filter. The expected value in the second term is non zero because of the common air receiver causes correlation in the measurement noise vectors $\mathbf{v}_1$ and $\mathbf{v}_2$. This term will be referred to as $\mathbf{V}_{12}$ and is basically the cross correlation between the measurement noises from the two tracks. Therefore, the resulting expression for the covariance at time *k* is

$$\begin{aligned}\hat{\mathbf{P}}_{y1y2,k} = &\left(\mathbf{I} - \mathbf{K}_{1,k}\mathbf{H}_{1,k}\right)\overline{\mathbf{P}}_{y1y2,k}\left(\mathbf{I} - \mathbf{K}_{2,k}\mathbf{H}_{2,k}\right)^T \\ &+ \mathbf{K}_{1,k}\mathbf{V}_{12,k}\mathbf{K}_{2,k}^T\end{aligned} \quad (21)$$

In Equation 21, $\mathbf{K}_{1,k}$, $\mathbf{K}_{2,k}$, $\mathbf{H}_{1,k}$ and $\mathbf{H}_{2,k}$ are all known from the individual Kalman filters that are implemented for each individual track. Detailed discussions of how to evaluate $\mathbf{V}_{12}$ and how to initialize the covariance propagation in Equation 21 are provided in Appendix B and Appendix C, respectively. Notice that in order to be able to use Equation 21 to compute $\hat{\mathbf{P}}_{y1y2}$ the full state vector (for example: position, ambiguities, multipath states, etc.) that is used in estimating the position in each individual filter is used.

Next, in order to derive a formula for $\overline{\mathbf{P}}_{y1y2,k}$, we start with the dynamic model and time update Kalman filter equations for $\mathbf{y}_1$ and $\mathbf{y}_2$, respectively:

$$\begin{aligned}\mathbf{y}_{1,k} &= \mathbf{F}_{1,k-1}\,\mathbf{y}_{1,k-1} + \mathbf{w}_{1,k-1} \\ \overline{\mathbf{y}}_{1,k} &= \mathbf{F}_{1,k-1}\,\hat{\mathbf{y}}_{1,k-1}\end{aligned} \quad (22)$$

$$\begin{aligned}\mathbf{y}_{2,k} &= \mathbf{F}_{2,k-1}\,\mathbf{y}_{2,k-1} + \mathbf{w}_{2,k-1} \\ \overline{\mathbf{y}}_{2,k} &= \mathbf{F}_{2,k-1}\,\hat{\mathbf{y}}_{2,k-1}\end{aligned} \quad (23)$$

where $\mathbf{F}_1$ and $\mathbf{F}_2$ are the dynamic transition matrices for $\mathbf{y}_1$ and $\mathbf{y}_2$, respectively. By definition, the cross covariance matrix $\overline{\mathbf{P}}_{y1y2,k}$ is

$$\overline{\mathbf{P}}_{y1y2,k} = E\left\{\left(\mathbf{y}_{1,k} - \overline{\mathbf{y}}_{1,k}\right)\left(\mathbf{y}_{2,k} - \overline{\mathbf{y}}_{2,k}\right)^T\right\} \quad (24)$$

Substituting Equations 22 and 23 in Equation 24:

$$\begin{aligned}\overline{\mathbf{P}}_{y1y2,k} = E\{&\left[\mathbf{F}_{1,k-1}\left(\mathbf{y}_{1,k-1} - \hat{\mathbf{y}}_{1,k-1}\right) + \mathbf{w}_{1,k-1}\right] \\ &\left[\mathbf{F}_{2,k-1}\left(\mathbf{y}_{2,k-1} - \hat{\mathbf{y}}_{2,k-1}\right) + \mathbf{w}_{2,k-1}\right]^T\}\end{aligned} \quad (25)$$

where $\mathbf{w}_1$ and $\mathbf{w}_2$ are the process noise vectors for states $\mathbf{y}_1$ and $\mathbf{y}_2$, respectively. Assuming that the process noise is independent from the estimates, Equation 25 can be further simplified to:

$$\begin{aligned}\overline{\mathbf{P}}_{y1y2,k} = &\mathbf{F}_{1,k-1}E\left\{\left(\mathbf{y}_{1,k-1} - \hat{\mathbf{y}}_{1,k-1}\right)\left(\mathbf{y}_{2,k-1} - \hat{\mathbf{y}}_{2,k-1}\right)^T\right\}\mathbf{F}_{2,k-1}^T \\ &+ E\left\{\mathbf{w}_{1,k-1}\,\mathbf{w}_{2,k-1}^T\right\}\end{aligned} \quad (26)$$

From Equation 18, the first expected value in the right hand side of Equation 26 is $\hat{\mathbf{P}}_{y1y2,k-1}$. The second expected value in Equation 26 is the cross covariance of the process noise between the two tracks, which will be referred to as $\mathbf{Q}_{12,k-1}$. Therefore, the Kalman filter time update (Equation 26) can be rewritten as

$$\overline{\mathbf{P}}_{y1y2,k} = \mathbf{F}_{1,k-1}\,\hat{\mathbf{P}}_{y1y2,k-1}\mathbf{F}_{2,k-1}^T + \mathbf{Q}_{12,k-1} \quad (27)$$

In Equation 27, the dynamic matrices $\mathbf{F}_1$ and $\mathbf{F}_2$ are known and already evaluated from the individual Kalman filter time updates. The evaluation of the cross covariance process noise $\mathbf{Q}_{12}$ is discussed in Appendix D.

Correlation Effects on the Averaging Approach

Comparing the measurement models in Equations 16 and 17 to Equations 8, 9 and 10 and utilizing Equations 21 and 27, the off diagonal block matrices of $\mathbf{R}_0$ in

Equation 13 can be evaluated. Remember, however, that Equations 21 and 27 provide the covariance of the state vector **y** (including all states, not only position **x**) and that only the position covariance is used in $\mathbf{R}_0$. Therefore, $\mathbf{R}_0$ is the 3×3 sub-matrix corresponding to the position states is extracted from $\hat{\mathbf{P}}_{y1y2,k}$.

Using weighted least squares estimation with Equation 12, $\hat{\mathbf{x}}_0$ and its covariance can be written as,

$$\hat{\mathbf{x}}_0 = \left(\mathbf{H}_0^T \mathbf{R}_0^{-1} \mathbf{H}_0\right)^{-1} \mathbf{H}_0^T \mathbf{R}_0^{-1} \mathbf{z}_0 \tag{28}$$

$$\mathbf{P}_{\mathbf{x}0} = \left(\mathbf{H}_0^T \mathbf{R}_0^{-1} \mathbf{H}_0\right)^{-1} \tag{29}$$

$\sigma_{v|H0}$ in Equation 4 that is used to evaluate VPL_{H0} is computed from the (3,3) element of $\mathbf{P}_{\mathrm{x}0}$ as $\sigma_{v|H0} = \sqrt{\mathbf{P}_{\mathbf{x}0(3,3)}}$.

Now that the H0 hypothesis calculation is done for the averaging method, attention is directed toward the H1*j* hypothesis. Remember that under the H1*j* hypothesis, the j^{th} receiver will be considered faulty and will not be used in the estimation of the averaged **x**. For example, for $j = 1$, receivers 2 and 3 are used to estimate an average estimate of the relative vector (referred to as $\hat{\mathbf{x}}_{1_j}$, where the first subscript means that is estimated under the H1 hypothesis and the second subscript defines which faulty receiver is being hypothesized). Similar to Equation 12, this can be modeled as (for an example case of $j = 1$),

$$\begin{bmatrix} \hat{\mathbf{x}}_2 + \mathbf{b}_2 \\ \hat{\mathbf{x}}_3 + \mathbf{b}_3 \end{bmatrix} = \begin{bmatrix} \mathbf{I} \\ \mathbf{I} \end{bmatrix} \mathbf{x}_{11} + \begin{bmatrix} \boldsymbol{\varepsilon}_{x2} \\ \boldsymbol{\varepsilon}_{x3} \end{bmatrix} \Rightarrow \mathbf{z}_{11} = \mathbf{H}_{11}\mathbf{x}_{11} + \mathbf{v}_{11} \tag{30}$$

with a measurement noise covariance matrix

$$\mathbf{R}_{11} = \begin{bmatrix} \hat{\mathbf{P}}_{x2x2} & \hat{\mathbf{P}}_{x2x3} \\ \hat{\mathbf{P}}_{x2x3}^T & \hat{\mathbf{P}}_{x3x3} \end{bmatrix} \tag{31}$$

All the block matrices in Equation 31 have already been evaluated in the process of computing $\hat{\mathbf{x}}_0$ described just above. As a result, $\hat{\mathbf{x}}_{11}$ can be estimated as,

$$\hat{\mathbf{x}}_{11} = \left(\mathbf{H}_{11}^T \mathbf{R}_{11}^{-1} \mathbf{H}_{11}\right)^{-1} \mathbf{H}_{11}^T \mathbf{R}_{11}^{-1} \mathbf{z}_{11} \tag{32}$$

with a covariance,

$$\mathbf{P}_{\mathbf{x}11} = \left(\mathbf{H}_{11}^T \mathbf{R}_{11}^{-1} \mathbf{H}_{11}\right)^{-1} \tag{33}$$

The 3rd element of the vectors $\hat{\mathbf{x}}_0$ and $\hat{\mathbf{x}}_{11}$ are extracted and subtracted then used to compute $|v_0 - v_{11}|$, while the (3,3) element of $\mathbf{P}_{\mathrm{x}11}$ is extracted to compute $\sigma_{v|H11}$ as

$$\sigma_{v|H11} = \sqrt{\mathbf{P}_{\mathbf{x}11(3,3)}} \tag{34}$$

With $|v_0 - v_{11}|$ and $\sigma_{v|H11}$ having been defined, VPL_{H11} can be computed using Equation 5. The same procedure can be followed to compute VPL_{H12} and VPL_{H13}.

Now that VPL_{H0} and VPL_{H1j} are evaluated, the only measure that is left is $PVPL_{H1j}$ (Equation 7). Therefore, it is necessary to derive a formula for computing $\sigma_{|v0-v1j|}$. For clarity in the development, but without the loss of generality, we will consider the case $j = 1$. Remember that estimation of $\mathbf{x}_0$ and $\mathbf{x}_{11}$ uses measurements from the same airborne receiver as well as common measurements for reference receivers 2 and 3. Therefore, $\hat{\mathbf{x}}_0$ and $\hat{\mathbf{x}}_{11}$ are correlated. Defining the cross covariance matrix between these two vectors as $\mathbf{P}_{\mathrm{x}0\mathrm{x}11}$, then the covariance of $\hat{\mathbf{x}}_0 - \hat{\mathbf{x}}_{11}$ ($\mathbf{P}_{\mathrm{x}0\text{-}\mathrm{x}11}$) can be written in terms of $\mathbf{P}_{\mathrm{x}0}$, $\mathbf{P}_{\mathrm{x}11}$ and $\mathbf{P}_{\mathrm{x}0\mathrm{x}11}$ as,

$$\mathbf{P}_{\mathbf{x}0-\mathbf{x}11} = \mathbf{P}_{\mathbf{x}0} - \mathbf{P}_{\mathbf{x}0\mathbf{x}11} - \mathbf{P}_{\mathbf{x}0\mathbf{x}11}^T + \mathbf{P}_{\mathbf{x}11} \tag{35}$$

Since both $\hat{\mathbf{x}}_0$ and $\hat{\mathbf{x}}_{11}$ are computed using least squares estimation equations (Equations 28 and 32), the estimate errors for $\hat{\mathbf{x}}_0$ and $\hat{\mathbf{x}}_{11}$ can be written as in Equations 36 and 37, respectively.

$$\hat{\mathbf{x}}_0 - \mathbf{x} = \left(\mathbf{H}_0^T \mathbf{R}_0^{-1} \mathbf{H}_0\right)^{-1} \mathbf{H}_0^T \mathbf{R}_0^{-1} \mathbf{v}_0 \tag{36}$$

$$\hat{\mathbf{x}}_{11} - \mathbf{x} = \left(\mathbf{H}_{11}^T \mathbf{R}_{11}^{-1} \mathbf{H}_{11}\right)^{-1} \mathbf{H}_{11}^T \mathbf{R}_{11}^{-1} \mathbf{v}_{11} \tag{37}$$

Therefore, by definition, $\mathbf{P}_{\mathrm{x}0\mathrm{x}11}$ is

$$\begin{aligned} \mathbf{P}_{x0x11} &= E\left\{\left(\hat{\mathbf{x}}_0 - \mathbf{x}\right)\left(\hat{\mathbf{x}}_{11} - \mathbf{x}\right)^T\right\} \\ &= \left(\mathbf{H}_0^T \mathbf{R}_0^{-1} \mathbf{H}_0\right)^{-1} \mathbf{H}_0^T \mathbf{R}_0^{-1} \mathbf{R}_{0,11} \mathbf{R}_{11}^{-1} \mathbf{H}_{11} \left(\mathbf{H}_{11}^T \mathbf{R}_{11}^{-1} \mathbf{H}_{11}\right)^{-1} \end{aligned} \tag{38}$$

where $\mathbf{R}_{0,11} = E\left\{\mathbf{v}_0 \mathbf{v}_{11}^T\right\}$ and $\mathbf{v}_0$ and $\mathbf{v}_{11}$ are defined by equations 12 and 30, respectively. Since the correlation between the individual estimates have already been evaluated, $\mathbf{R}_{0,11}$ (a non-square cross covariance matrix) can be easily extracted from $\mathbf{R}_0$. In this case for example, the expression for $\mathbf{R}_{0,11}$ becomes,

$$\mathbf{R}_{0,11} = E\left\{\begin{bmatrix} \boldsymbol{\varepsilon}_{x1} \\ \boldsymbol{\varepsilon}_{x2} \\ \boldsymbol{\varepsilon}_{x3} \end{bmatrix} \begin{bmatrix} \boldsymbol{\varepsilon}_{x2} & \boldsymbol{\varepsilon}_{x3} \end{bmatrix}\right\} = \begin{bmatrix} \hat{\mathbf{P}}_{\mathbf{x}1\mathbf{x}2} & \hat{\mathbf{P}}_{\mathbf{x}1\mathbf{x}3} \\ \hat{\mathbf{P}}_{\mathbf{x}2\mathbf{x}2} & \hat{\mathbf{P}}_{\mathbf{x}2\mathbf{x}3} \\ \hat{\mathbf{P}}_{\mathbf{x}3\mathbf{x}2} & \hat{\mathbf{P}}_{\mathbf{x}3\mathbf{x}3} \end{bmatrix} \tag{39}$$

Comparing the result in Equation 39 with the expression of $\mathbf{R}_0$ in Equation 13, it is noticed that $\mathbf{R}_{0,11}$ is $\mathbf{R}_0$ with the first block-column removed. Notice that the first block-column in this case corresponds to the faulty receiver. As a result, $\mathbf{P}_{\mathrm{x}0\text{-}\mathrm{x}11}$ in Equation 35 can be computed and $\sigma_{|v0-v11|}$ is evaluated as

$$\sigma_{|v0-v11|} = \sqrt{\mathbf{P}_{\mathbf{x}0-\mathbf{x}11,(3,3)}} \tag{40}$$

Following a similar procedure to compute $\sigma_{|v0-v1j|}$ for any receiver *j*, $PVPL_{H1j}$ can be computed for all reference receivers using Equation 7.

Since all components of the H1 algorithm (VPL_{H0}, VPL_{H1j} and $PVPL_{H1j}$) have been evaluated for the averaging method, the following section will discuss deriving similar expressions for the coupled estimation method.

IV. COUPLED ESTIMATION APPROACH

In the coupled estimation approach, measurements from different reference receivers are translated to a single reference receiver using the lever arm information and the attitude of the ship. By combining these measurements at one common reference point, a single relative position vector is estimated. Directly incorporating the geometry constraint prior to fixing the cycle ambiguities results in improved cycle ambiguity observability [15]. In this work, measurements from different reference receivers are assumed to be independent. Returning to Equations 8, 9 and 10 and replacing $\mathbf{x}_1$, $\mathbf{x}_2$ and $\mathbf{x}_3$ by $\mathbf{x} - \mathbf{b}_1$, $\mathbf{x} - \mathbf{b}_2$ and $\mathbf{x} - \mathbf{b}_3$, respectively, and combining them into a single measurement model, we have

$$\begin{bmatrix} \nabla\Delta\boldsymbol{\varphi}_1 + \Delta\mathbf{e}^T\mathbf{b}_1 \\ \nabla\Delta\boldsymbol{\varphi}_2 + \Delta\mathbf{e}^T\mathbf{b}_2 \\ \nabla\Delta\boldsymbol{\varphi}_3 + \Delta\mathbf{e}^T\mathbf{b}_3 \end{bmatrix} = \begin{bmatrix} \Delta\mathbf{e}^T & \lambda\mathbf{I} & \mathbf{0} & \mathbf{0} \\ \Delta\mathbf{e}^T & \mathbf{0} & \lambda\mathbf{I} & \mathbf{0} \\ \Delta\mathbf{e}^T & \mathbf{0} & \mathbf{0} & \lambda\mathbf{I} \end{bmatrix} \begin{bmatrix} \mathbf{x} \\ \nabla\Delta\mathbf{N}_1 \\ \nabla\Delta\mathbf{N}_2 \\ \nabla\Delta\mathbf{N}_3 \end{bmatrix} + \begin{bmatrix} \boldsymbol{\varepsilon}_{\Delta\phi 1} \\ \boldsymbol{\varepsilon}_{\Delta\phi 2} \\ \boldsymbol{\varepsilon}_{\Delta\phi 3} \end{bmatrix} \tag{41}$$

Because the same airborne receiver is used, the double difference carrier phase measurement noise vectors $\boldsymbol{\varepsilon}_{\Delta\phi 1}$, $\boldsymbol{\varepsilon}_{\Delta\phi 2}$ and $\boldsymbol{\varepsilon}_{\Delta\phi 3}$ are correlated. The associated measurement noise matrix accounting for this correlation is derived in Appendix B. As a result, $\mathbf{x}$ can be estimated using a Kalman filter. Going back to the multiple-receiver case: in a fault free mode (H0), with all receivers being operational, measurements from all receivers are processed in a similar form as in Equation 41 and $\hat{\mathbf{x}}_0$ and $\mathbf{P}_{x0}$ are estimated using a single Kalman filter. For the H1*j* case, measurements from all receivers except the j^{th} receiver are used in a similar fashion to estimate $\hat{\mathbf{x}}_{1j}$ and $\mathbf{P}_{x1j}$.

Having $\hat{\mathbf{x}}_0$, $\hat{\mathbf{x}}_{1j}$, $\mathbf{P}_{x0}$, and $\mathbf{P}_{x1j}$, VPL_{H0} and VPL_{H1j} are computed as explained in the averaging section. As discussed before, the computation of $PVPL_{H1j}$ requires evaluating $\sigma_{|v0-v11|}$. Equations (35) and (40) can be used to evaluate $\sigma_{|v0-v11|}$. The difference between the averaging and coupled approach is in computing $\mathbf{P}_{x0x1j}$. In Equation (38), a formula for computing $\mathbf{P}_{x0x1j}$ was derived based on the fact that $\hat{\mathbf{x}}_0$ and $\hat{\mathbf{x}}_{1j}$ are estimated using least squares estimation. In the coupled estimation approach, both $\hat{\mathbf{x}}_0$ and $\hat{\mathbf{x}}_{1j}$ are estimated using Kalman filters with the same airborne receiver and some common reference receivers (all except for the j^{th} receiver). Recall, however, that a methodology to generate the cross covariance of two correlated Kalman filter estimates has been developed in the previous section. Therefore, Equations (21) and (27) can be used again to obtain $\mathbf{P}_{x0x1j}$.

Sections II, III and IV (and the appendices) provided a detailed derivation of the H1 algorithm for two different approaches toward using redundant reference receiver measurements. In order to investigate the advantages and disadvantages of each approach more thoroughly, an availability analysis for an example shipboard aircraft landing application is conducted.

V. AVAILABILITY ANALYSIS

In this section, the H0 and H1 performance of a high accuracy and integrity navigation system is quantified through availability analysis. An example of the navigation algorithms that were developed for autonomous airborne refueling and autonomous shipboard landing in [3], [6] and [11] is used as a baseline navigation architecture for reference receiver failure detection and mitigation. Next is a summary of the underlying concept of these algorithms. More details can be found in [3], [6] and [11]. The GPS navigation algorithm for these applications performs geometry free/divergence free code-carrier filtering continuously for visible satellites on both the aircraft and the reference station until the aircraft is close to the reference station [3] and [6] . A geometry free observable [16], by definition, does not depend on the geometry of the satellites or the user location and eliminates all error sources except for receiver noise and multipath. A geometry free measurement of the widelane cycle ambiguity is formed by subtracting the narrowlane pseudorange from the widelane carrier phase [10] and [16]. A drawback of the geometry free measurement is the presence of higher noise relative to the L1 and L2 carrier phase measurements. This can be overcome by filtering the geometry free measurement over time prior to the final approach. In order to model colored multipath noise in the geometry free measurements and Kalman filter, a first

order Gauss-Markov measurement error model is used. The outputs of the filtering process are the floating widelane cycle ambiguity estimates. When the aircraft is close to the ship (or tanker) L1/L2 cycle ambiguity estimates can be extracted with the aid of the satellite geometric redundancy [3], [4] and [6]. Next, the cycle ambiguities are fixed using the bootstrap method [17]. The bootstrap rounding process is performed for those ambiguities that can be fixed with a probability of incorrect fix (PIF) that is compliant with the fault free integrity risk requirement. The remaining ambiguities remain floating. As a result, it is clear that all these differences between GBAS (which relies solely on point positioning using carrier smoothed code measurements) and the high accuracy carrier phase navigation algorithm under investigation present tremendous challenges in H1 mitigation.

The described navigation architecture is used as a basis to determine the covariance of the position estimate error. Using both the averaging and coupled estimation approaches as discussed in Sections III and IV, this covariance is then used to compute $\sigma_{v|H0}$, $\sigma_{v|H1j}$ and $\sigma_{|v0-v1j|}$ for each of the two methods. Next, *VPL* is evaluated based on the values and relations in Section II and compared to VAL. In order to account for the GPS satellite geometry change (which is repeatable every day), availability analysis is performed by simulating 1440 satellite geometries (one geometry per minute during the day). Availability is then calculated as the percentage of cases (geometries) for which *VPL* is less than *VAL*.

H0 and H1 availability for the averaging approach is compared to the coupled estimation approach for two scenarios, depending on the number of reference receivers that are installed in the ship: either two or three reference receivers. In addition, availability in the case where the ship is equipped with a single reference receiver is evaluated as a baseline for comparison. In each of these scenarios, a single airborne receiver is assumed. The requirements and simulation parameters that are used in evaluating the availability are not necessarily the requirements that are used currently in the shipboard landing navigation system. Nevertheless, representative example requirements are chosen based on those given in [6], [11] and [18] (Table 1). In this simulation, the standard deviation of the carrier phase (single difference) measurement noise $\sigma_{\Delta\phi}$ and single difference pseudorange code $\sigma_{\Delta PR}$ are assumed to be 1 cm and 50 cm, respectively. The single difference standard deviations $\sigma_{\Delta PR}$ and $\sigma_{\Delta\phi}$ are related to the raw values (σ_{PR} and σ_{ϕ}) by a scaling factor of $\sqrt{2}$. In this analysis, to simulate an actual aircraft mission with significant banking, a maximum airborne prefiltering period of 5 minutes for the geometry free observables is used to generate floating estimates of the widelane cycle ambiguities. In other words, if the satellite has been visible by the aircraft for a period of time longer than the maximum prefiltering time, the prefiltering time is set to the maximum prefiltering time. In contrast, because ship maneuvers are much less aggressive, the maximum prefiltering time is set to the time since the satellite first came in view. The remaining simulation parameters are summarized in Table 1.

Table 1: Simulation Parameters

Parameter	Value
$P_v(MI\|H0)$	10^{-7}
K_{ffmd}	5.327
P(H1j)	10^{-5}
K_{md}	2.170
Continuity risk req.	10^{-6}
K_{ffc}	4.892
VAL	1.8 m
Satellite constellation	Almanac of May 15 2007
Location	Atlantic Ocean (27°N and 74°W)
Maximum airborne prefiltering time	5 minutes
Aircraft multipath Gauss Markov time constant	20 seconds
Ship multipath Gauss Markov time constant	60 seconds

Using the parameters detailed in Table 1, a covariance analysis simulation is performed and availability is calculated. Table 2 shows the availability results for both methods using different numbers of reference receivers. For the H0 case, the averaged method outperforms the single reference receiver case by 9% (for two receivers) to 18% (three receivers). The performance of the coupled estimation method, on the other hand, is superior to the averaging method: the additional availability gain is approximately 19% for two antennas and 15% for three antennas. This gain in availability is attributed to cycle resolution enhancement provided by the coupled estimation method.

Based on the development in Sections III and IV, it is evident that the implementation of the H0 algorithm in the averaged estimation method is more complicated than that in the coupled estimation method. In the coupled estimation, a single Kalman filter (KF) for the fused measurements from different antennas is used to estimate the relative position vector. In the averaging method with two antennas for example, two Kalman filters are required to estimate the two individual vectors with a third Kalman filter (covariance propagation only) to estimate the correlation between the two individual estimates due to common airborne receiver. Furthermore, an additional least squares (LS) estimation process is used to average the two individual estimates.

Table 2: Availability Results

		H0 Availability	H1 Availability
	1 Rcvr.	65.0 %	0 %
Averaged	2 Rcvr.	74.5 %	74.5 %
	3 Rcvr.	83.2 %	83.2 %
Coupled	2 Rcvr.	95.4 %	93.7 %
	3 Rcvr.	97.9 %	97.9 %

The performance of the algorithms is also evaluated under the H1 hypothesis. For a single reference receiver, the availability is zero regardless of the integrity requirement because the continuity requirement cannot be fulfilled (the 10^{-5} probability of reference receiver failing is greater than the continuity risk requirement of 10^{-6}). In the multi-receiver case, the results in Table 2 show that the H1 hypothesis has little impact on availability compared to H0. This is explained by the fact that for this application and the parameters in Table 1, the accuracy requirement [approximately σ_v = 20 cm (corresponding to 95% accuracy requirement of 40 cm)] is a more stringent availability driver than the fault free integrity requirement (σ_v on the order of 34 cm), and the choice of integrity method is not limiting availability. Since H1 hypothesis affects integrity and not accuracy, availability was not greatly affected. Overall, the coupled estimation provides the overall optimal performance in terms of availability, accuracy and integrity compared to single receiver and to the averaging method that was used in GBAS.

Unfortunately, the performance enhancement using the coupled estimation method comes with a cost. Table 3 shows the number of states and measurements (assuming 12 visible satellites with L1/L2 measurements) that are required for the cases in Table 2. These numbers have an impact on the computation time and memory allocation for each of these algorithms, which can be crucial for real time implementation. Remember that an inversion of a matrix with size equal to the measurement vectors is necessary in the Kalman filter. Also, matrix sizes are based on both the number of measurements and the number of states. For example, for the three reference receiver case, although the coupled estimation under the H0 hypothesis provides the best performance for three antennas, the coupled Kalman filter is composed of 66 double difference L1/L2 carrier phase measurements and 135 states: 3 states for position, 66 states for double difference L1/L2 ambiguities and 66 for double difference multipath states. On the other hand, each of the six individual Kalman filters in the averaging method has only 22 measurements and 45 states. Furthermore, extra least squares estimation computations are also necessary in the averaging method, the size of the least squares estimation for three antennas is small (9×9) compared to the Kalman filter.

Different techniques can be introduced to increase the computation efficiency of coupled estimation by reducing the number of states and reducing the number of measurements per Kalman filter measurement update. These techniques are not discussed in this paper, but a few examples are mentioned as alternatives in order to enhance the computation efficiency. Examples of these techniques include the UD Kalman filter [19] and the measurement differencing Kalman filter [20] and [21]. Another alternative is to perform the measurement updates for uncorrelated measurements separately in the Kalman filter, which reduces the size of the computation load in the matrix inversion. For example, under the assumption that L1 and L2 measurement errors are uncorrelated, L1 and L2 measurement updates can be performed individually. Currently, a real time implementation of these algorithms is underway to quantitatively evaluate the computational efficiency of the algorithms.

Table 3: Number of Kalman filters and least squares including number of measurements and states required for implementation.

		Averaged		Coupled	
		2 Rcvr.	3 Rcvr.	2 Rcvr.	3 Rcvr.
H0	No. of KF	3	6	1	1
	States/Meas.	47/22	47/22	91/44	135/66
	No. of LS/states	1/6	1/9	0	0
H1 (only)	No. of KF	0	0	4	6
	States/Meas.	0	0	47/22	91/44
	No. of LS/states	2/6	6/9	0	0

CONCLUSIONS

A general methodology to mitigate single receiver failures for carrier phase navigation architectures was developed. Two different approaches to utilize redundant carrier phase measurements from multiple reference receivers were described: an averaging approach and coupled estimation approach. The impact of using these different methods on accuracy and integrity was investigated. The navigation performance, measured by availability under both the fault free and single receiver failure hypotheses, was shown to be superior for the coupled estimation when compared to the averaging method. Different perspectives, such as implementation complexity and computational efficiency, have also been discussed for both approaches. Although the coupled estimation is relatively easier to implement than the averaging method, it might require more computational power.

APPENDIX A: VPL FORMULA DERIVATION

This appendix provides the derivation of the VPL formulas that are used in this paper. *VPL* is defined as a statistical overbound where the probability of the vertical position estimate error ($|v-\hat{v}|$) exceeding *VPL* equals the associated integrity risk requirement (I_{req}) (42).

$$P\{|v-\hat{v}|>VPL\}=I_{req} \tag{42}$$

where,

P{·} is the probability of event ·

$\hat{v}$ is the vertical component of the estimated relative position vector

v is the vertical component of the true relative position vector

I_{req} is the integrity risk requirement, which can represent either the H0 or H1 integrity allocations.

Fault-free measurements are assumed to be unbiased. The Kalman filter, which is used for position estimation in this work, is a maximum likelihood estimator. Therefore, using fault-free measurements, the estimates are unbiased and represent the best knowledge of the true relative position vector. In other words, the vertical component of the true relative position vector v can be written in terms of $\hat{v}_{H0|0}$, the vertical component of the relative position estimate using the H0 estimator (which assumes no receiver faults) and given that no receiver has actually failed,

$$v=\hat{v}_{H0|0}+\delta\hat{v}_{H0|0} \tag{43}$$

where $\delta\hat{v}_{H0|0}$ is the error in this vertical estimate. In this case, distribution of the estimate error $v-\hat{v}=\delta\hat{v}_{H0|0}$ is bounded by a Gaussian distribution with a zero mean and a standard deviation $\sigma_{v|H0}$. Since Equation 42 represents the two-sided tail probability, it can be simplified in terms of the Gaussian cumulative distribution function (Φ) with one-sided tail to

$$\Phi\left(-\frac{VPL_{H0}}{\sigma_{v|H0}}\right)=\frac{I_{H0req}}{2} \tag{44}$$

where, VPL_{H0} and I_{H0req} are the VPL and integrity risk allocation under the H0 hypothesis, respectively.

Solving for VPL_{H0} in (44) results in

$$VPL_{H0}=-\Phi^{-1}\left(\frac{I_{H0req}}{2}\right)\sigma_{v|H0}=K_{ffmd}\,\sigma_{v|H0} \tag{45}$$

where $\Phi^{-1}\left(\frac{I_{H0req}}{2}\right)=\sqrt{2}\,\mathrm{erf}\left(I_{H0req}-1\right)$, and therefore $K_{ffmd}=-\sqrt{2}\,\mathrm{erf}\left(I_{H0req}-1\right)$.

VPL_{H1j} can be derived in a similar fashion to VPL_{H0}. However, VPL_{H1j} represents a statistical overbound on the vertical position estimate error under the hypothesis that receiver j has failed. If an erroneous measurement from the j^{th} receiver is used in estimating the relative position vector, it is expected that it will induce a bias (μ) in the vertical component of that estimate. Therefore, the vertical position estimate using the nominal H0 estimator [i.e., using all receivers including the j^{th} receiver ($\hat{v}_{H0|j}$)] will be biased and Equation 43 can be rewritten as,

$$v=\hat{v}_{H0|j}+\delta\hat{v}_{H0|j} \tag{46}$$

In this case, the estimate error under the H0 hypothesis given that the j^{th} receiver has failed $v-\hat{v}_{H0|j}=\delta\hat{v}_{H0|j}$ is biased. In order to obtain an estimate of this bias, consider the case where the vertical position vector is estimated after excluding the j^{th} receiver ($\hat{v}_{1j}$). The true vertical component of the position vector in this case becomes

$$v=\hat{v}_{H1j|j}+\delta\hat{v}_{H1j|j} \tag{47}$$

By subtracting $\hat{v}_{H0|j}$ from both sides of Equation (47) and solving for $\delta\hat{v}_{H0|j}$ [defined in (43)],

$$v-\hat{v}_{H0|j}=\delta\hat{v}_{H0|j}=\hat{v}_{H1j|j}-\hat{v}_{H0|j}+\delta\hat{v}_{H1j|j} \tag{48}$$

In this case, the estimate error under H_{1j} ($\delta\hat{v}_{H0|j}$) in (48) is composed of a random term ($\delta\hat{v}_{H1j|j}$) and a

deterministic term ($\hat{v}_{H1|j|j} - \hat{v}_{H0|j}$) that represents the bias (μ). The term $\delta\hat{v}_{H1|j|j}$ has a Gaussian distribution with zero mean (because it is fault-free) and a standard deviation $\sigma_{v|H1j}$. Therefore, VPL_{H1j} is computed for a biased Gaussian distribution with a mean of μ and sigma of $\sigma_{v|H1j}$. We will now derive the formula to evaluate VPL_{H1j} for any mean μ and replace it by the term $\hat{v}_{H1|j|j} - \hat{v}_{H0|j}$ afterwards.

From the definition of *VPL* in (42) and with a biased Gaussian distribution, VPL_{H1j} can be formulated as

$$P\left\{\left|v-\hat{v}\right| > VPL_{H1j} \mid H1j\right\} = I_{H1jreq} \tag{49}$$

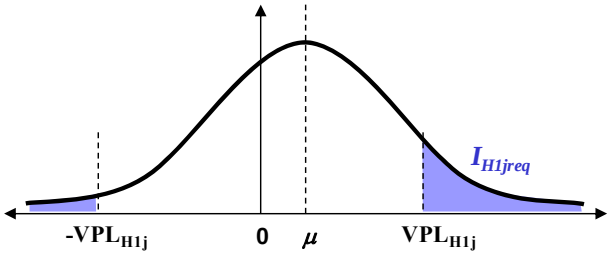

Figure 2: A schematic representation of a biased Gaussian distribution including the area that represents the integrity risk requirement I_{H1jreq}.

From Figure 2, Equation 49 can be written in terms of Φ as,

$$\Phi\left(\frac{-VPL_{H1j}-\mu}{\sigma_{v|H1j}}\right) + 1 - \Phi\left(\frac{VPL_{H1j}-\mu}{\sigma_{v|H1j}}\right) = I_{H1jreq} \tag{50}$$

Although, it is quite difficult to solve for VPL_{H1j} analytically from (50), a conservative quantity can be derived. Consider first the case where μ is positive as in Figure 2. In that case, the area of I_{H1jreq} that is under the positive tail will always be larger than the one under the negative tail. Also, it can be easily shown that the area under the positive tail corresponding to I_{H1jreq} is larger than half of the total area of I_{H1jreq}. Therefore, as illustrated in Figure 3, (50) can be simplified and converted to a one-sided tail with $I_{H1jreq}/2$ and used to compute a conservative value for VPL_{H1j} as,

$$1 - \Phi\left(\frac{VPL'_{H1j}-\mu}{\sigma_{v|H1j}}\right) = \frac{I_{H1jreq}}{2} \tag{51}$$

which can be used to solve for the conservative VPL'_{H1j} (52).

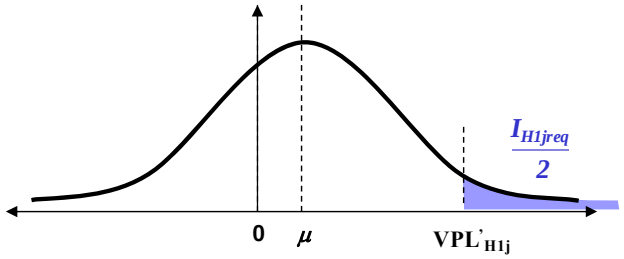

Figure 3: A schematic representation of the conservative VPL'_{H1j} that is based on one sided tail probability of $I_{H1jreq}/2$.

$$\begin{aligned} VPL'_{H1j} &= \mu - \Phi^{-1}\left(\frac{I_{H1jreq}}{2}\right)\sigma_{v|H1j} \\ &= \mu + K_{md}\,\sigma_{v|H1j} \end{aligned} \tag{52}$$

where $K_{md} = -\Phi\left(\frac{I_{H1jreq}}{2}\right) = -\sqrt{2}\,\mathrm{erf}\left(I_{H1jreq} - 1\right)$

For negative μ, the same logic can be followed, and VPL'_{H1j} in that case becomes $VPL'_{H1j} = -\mu + K_{md}\,\sigma_{v|H1j}$. As a result, for any value of μ, VPL_{H1j} can be written as,

$$VPL_{H1j} = |\mu| + K_{md}\,\sigma_{v|H1j} \tag{53}$$

Hence, substituting $\hat{v}_{H1|j|j} - \hat{v}_{H0|j}$ (or $\hat{v}_{1j} - \hat{v}_0$ as a shorthand notation) for μ [derived from (48)], *VPL* under the H1j hypothesis becomes

$$VPL_{H1j} = \left|\hat{v}_0 - \hat{v}_{1j}\right| + K_{md}\,\sigma_{v|H1j} \tag{54}$$

In summary, Equations (45) and (54) can be used to compute VPL_{H0} and VPL_{H1j}, respectively.

APPENDIX B: COVARIANCE OF THE CORRELATED MEASUREMENT NOISE $\mathbf{V}_{12}$

$\mathbf{V}_{12}$ is defined in Equations 20 and 21 as the cross correlation between the two measurement noise vectors $\mathbf{v}_1$ and $\mathbf{v}_2$. However, $\mathbf{v}_1$ and $\mathbf{v}_2$ are simplified notations for the double difference carrier phase measurements for tracks 1 and 2. For example, a single element of $\mathbf{v}_1$ can be expanded in terms of the raw carrier phase measurement noise (ε_ϕ) from reference receiver 1, air receiver *a*, satellite *k*, and reference satellite *l* as:

$$v_1 = \varepsilon^k_{\phi 1} - \varepsilon^k_{\phi a} - \varepsilon^l_{\phi 1} + \varepsilon^l_{\phi a} \tag{55}$$

Throughout the derivation of $\mathbf{V}_{12}$, the following assumptions will be used:

1- Measurement noises from different reference receivers are independent (uncorrelated).
2- Measurement noises from different satellites are independent (uncorrelated).

Therefore, the single difference operation (between ship and air receivers) can be written in a matrix form as,

$$\mathbf{v}_1' = \begin{bmatrix}\mathbf{A}_1 & -\mathbf{B}_1\end{bmatrix}\begin{bmatrix}\boldsymbol{\varepsilon}_{\phi 1}\\ \boldsymbol{\varepsilon}_{\phi a}\end{bmatrix} \tag{56}$$

where $\boldsymbol{\varepsilon}_{\phi 1}$ and $\boldsymbol{\varepsilon}_{\phi a}$ are the full vectors of the carrier phase measurement noise for reference receiver-1 and the airborne receiver, respectively. $\mathbf{A}_1$ and $\mathbf{B}_1$ are the matrices that extract the common visible satellites from reference receiver-1 and air measurements. For example, if both receivers (reference-1 and airborne) are tracking the same satellites, then both $\mathbf{A}_1$ and $\mathbf{B}_1$ would be identity matrices.

The double difference operation for the first track is accomplished by multiplying it with a double difference conversion matrix ($\mathbf{J}_1$) as,

$$\mathbf{v}_1 = \mathbf{J}_1\mathbf{v}_1' = \mathbf{J}_1\begin{bmatrix}\mathbf{A}_1 & -\mathbf{B}_1\end{bmatrix}\begin{bmatrix}\boldsymbol{\varepsilon}_{\phi 1}\\ \boldsymbol{\varepsilon}_{\phi a}\end{bmatrix} \tag{57}$$

$\mathbf{J}_1$ is composed of an identity matrix with the row corresponding to the reference satellite being removed, and the elements in the column corresponding to the reference satellite being replaced by -1. For example, if five satellites are tracked and the reference satellite is chosen to be the third one, $\mathbf{J} = \begin{bmatrix}1 & 0 & -1 & 0 & 0\\ 0 & 1 & -1 & 0 & 0\\ 0 & 0 & -1 & 1 & 0\\ 0 & 0 & -1 & 0 & 1\end{bmatrix}$.

If the same representation is followed for the second track, the measurement $\mathbf{v}_2$ can be written as:

$$\mathbf{v}_2 = \mathbf{J}_2\begin{bmatrix}\mathbf{A}_2 & -\mathbf{B}_2\end{bmatrix}\begin{bmatrix}\boldsymbol{\varepsilon}_{\phi 2}\\ \boldsymbol{\varepsilon}_{\phi a}\end{bmatrix} \tag{58}$$

From Equations 20 and 21, $\mathbf{V}_{12}$ is defined as:

$$\mathbf{V}_{12} = E\left\{\mathbf{v}_1\mathbf{v}_2^T\right\} \tag{59}$$

which can be written in terms of quantities in Equations 57 and 58, and using assumptions 1 and 2 above, as

$$\begin{aligned}\mathbf{V}_{12} &= E\left\{\mathbf{J}_1\begin{bmatrix}\mathbf{A}_1 & -\mathbf{B}_1\end{bmatrix}\begin{bmatrix}\boldsymbol{\varepsilon}_{\phi 1}\\ \boldsymbol{\varepsilon}_{\phi a}\end{bmatrix}\begin{bmatrix}\boldsymbol{\varepsilon}_{\phi 2}^T & \boldsymbol{\varepsilon}_{\phi a}^T\end{bmatrix}\begin{bmatrix}\mathbf{A}_2^T\\ -\mathbf{B}_2^T\end{bmatrix}\mathbf{J}_2^T\right\}\\ &= \mathbf{J}_1\mathbf{B}_1 E\left\{\boldsymbol{\varepsilon}_{\phi a}\boldsymbol{\varepsilon}_{\phi a}^T\right\}\mathbf{B}_2^T\mathbf{J}_2^T = \mathbf{J}_1\mathbf{B}_1\mathbf{V}_{\phi a}\mathbf{B}_2^T\mathbf{J}_2^T\end{aligned} \tag{60}$$

where $\mathbf{V}_{\phi a}$ is the measurement covariance matrix for the airborne carrier phase measurements.

APPENDIX C: INITIAL $\overline{\mathbf{P}}_{y1y2,0}$

The initial covariance $\overline{\mathbf{P}}_{y1y2,0}$ is the cross covariance between the initial estimates $\hat{\mathbf{y}}_1$ and $\hat{\mathbf{y}}_2$, where $\mathbf{y}_1$ and $\mathbf{y}_2$ might not only be the position states, but all estimated states as mentioned in Section III. From Equation 21, $\overline{\mathbf{P}}_{y1y2,0}$ is defined as $\overline{\mathbf{P}}_{y1y2,0} = E\left\{\left(\mathbf{y}_{1,0} - \overline{\mathbf{y}}_{1,0}\right)\left(\mathbf{y}_{2,0} - \overline{\mathbf{y}}_{2,0}\right)^T\right\}$. Therefore, the initial $\overline{\mathbf{P}}_{y1y2,0}$ depends on the type of state that is initialized and the value it is initialized to within the Kalman filter. The following are some examples of estimated states that are frequently used in GPS algorithms with their corresponding initial $\overline{\mathbf{P}}_{y1y2,0}$:

- Position states: Remember that the true position states are the same for both tracks (by definition). Therefore, if the two tracks are initialized similarly, say with zero value and a covariance **P**, then the elements of $\overline{\mathbf{P}}_{y1y2,0}$ corresponding to the position states will also be **P** (due to total correlation).

- Ambiguity states: the true ambiguities are generally different for different receivers. However, the elements of $\overline{\mathbf{P}}_{y1y2,0}$ corresponding to the ambiguity states depend on how the ambiguities are initialized in the individual filters. For example, if they are initialized with zero values and infinitely large covariance, then the covariance of the ambiguities in $\overline{\mathbf{P}}_{y1y2,0}$ is zero because they are not correlated. If the ambiguities are initialized with the carrier minus code measurements and the associated covariance, then the ambiguity elements of $\overline{\mathbf{P}}_{y1y2,0}$ are the correspondent covariance of the measurement noise between the individual tracks (taking the airborne measurement error correlation into account). This covariance matrix can be built following similar procedure to the one detailed in Appendix B but for the carrier-minus-code measurement noise instead of the carrier noise.

- Multipath states: the multipath colored error is usually modeled as first order Gauss Markov process. The single difference multipath states from the two tracks are therefore correlated due to the existence of the same air antenna. Therefore, the initial $\overline{\mathbf{P}}_{y1y2,0}$ for the multipath states is correlated in a similar fashion as the measurements

(following a similar procedure to the one in Appendix B).

- Atmospheric model states (ionospheric gradient and tropospheric refractivity index states): the true states in these cases are identical for both tracks (the air antenna and the reference antennas are usually within a short distance where atmospheric errors are totally correlated). Therefore, if these states are initialized with the same values in both tracks, (which is the case, and they are usually initialized with a value of zero), then $\overline{\mathbf{P}}_{y1y2,0}$ for these states is totally correlated for the same satellites (the covariance elements will be identical to the ones for each individual track).

APPENDIX D: COVARIANCE OF THE CORRELATED PROCESS NOISE Q_{12}

The cross covariance process noise $\mathbf{Q}_{12}$ in Equation 27 is defined as the covariance between process noises on the states for tracks 1 and 2. Therefore, the terms in $\mathbf{Q}_{12}$ will depend on the type of the process noise in each state. The following are examples of states used frequently in different GPS navigation applications:

- Position states: under the assumption that no attitude or lever arm errors exist in transforming both relative position vectors to the TDP, the true relative position and state dynamic for both tracks are the same. Therefore, the process noise on both tracks is the same as well. As a result, the process noise for the position states is totally correlated and the covariance elements in $\mathbf{Q}_{12}$ are identical to the individual process noise matrices.

- Multipath states: the covariance of the process noise for the multipath states depends on the multipath model used. For example, if a first order Gauss Markov model is used, then it is related to the multipath error standard deviation. The value of this standard deviation for the two tracks is correlated due to using the same air receiver (same air multipath). Therefore, the correlated process noise covariance can be evaluated in a similar fashion to the measurement noise $\mathbf{V}_{12}$ in Appendix B.

- Cycle ambiguity and atmospheric states: the covariance of the process noise for the ambiguity state is zero. Therefore, the elements of $\mathbf{Q}_{12}$ corresponding to these states are set to zero. Since the mission duration for shipboard applications is short compared to the time constant of atmospheric errors, an atmospheric state model similar to the one in [11] can be used. In that case, the process noise on these states in the individual tracks is assumed to be zero. Therefore, the elements of $\mathbf{Q}_{12}$ corresponding to these states are also zero.

ACKNOWLEDGEMENT

The authors gratefully acknowledge the Naval Air Systems Command (NAVAIR) of the US Navy for supporting this research. The authors would like to specifically acknowledge the support and guidance of Glenn Colby and Marie Lage regarding this work. However, the opinions discussed here are those of the authors and do not necessarily represent those of the U.S. Navy or any other affiliated agencies.

REFERENCES

[1] "Minimum Aviation System Performance Standards for the Local Area Augmentation System Airborne Equipment," *RTCA Document Number DO-245A,* December 2004.

[2] J. Hansen, G. Romrell, N. Nabaa, R. Andersen, L. Myers, and J. McCormick, "DARPA Autonomous Airborne Refueling Demonstration Program with Initial Results," *Proceedings of the 19th International Technical Meeting of the Satellite Division of the Institute of Navigation ION GNSS 2006*, Fort Worth, TX, Sep. 2006.

[3] S. Khanafseh and B. Pervan. "Autonomous Airborne Refueling of Unmanned Air Vehicles Using the Global Positioning System," *Journal of Aircraft,* Vol. 44, No. 5, Sep.-Oct. 2007.

[4] S. Dogra, J. Wright, and J. Hansen, "Sea-Based JPALS Relative Navigation Algorithm Development," *Proceedings of the 18th International Technical Meeting of the Satellite Division of the Institute of Navigation ION GNSS 2005*, Long Beach, CA, Sept. 2005.

[5] S. Wu, S. Peck and R. Fries, "Geometry Extra-Redundant Almost Fixed Solutions: A High Integrity Approach for Carrier Phase Ambiguity Resolution for High Accuracy Relative Navigation," *Proceeding of the IEEE/ION Position, Location, and Navigation Symposium (PLANS '2008)*, Monterey, CA, Apr. 2008.

[6] M. Heo, B. Pervan, S. Pullen, J. Gautier, P. Enge, and D. Gebre-Eziabher, "Robust Airborne Navigation Algorithm for SRGPS," *Proceedings of IEEE/ION Position, Location, and Navigation Symposium (PLANS '2004),* Monterey, CA, Apr. 2004.

[7] B. Pervan, S. Pullen, and J. Christie, "A Multiple Hypothesis Approach to Satellite Navigation Integrity," *NAVIGATION: Journal of Institute of Navigation,* vol. 45, No. 1, Spring 1998.

[8] F. Liu, T. Murphy, and T. Skidmore, "LAAS Signal-in-Space Integrity Monitoring

Description and Verification Plan," *Proceedings of the 10th International Technical Meeting of the Satellite Division of the Institute of Navigation ION GPS 1997*, Kansas City, MO, Sept. 1997.

[9] D. Kim and R. Langley, "GPS Ambiguity Resolution and Validation: Methodologies, Trends and Issues," *Proceedings of 7th GNSS Workshop - International Symposium on GPS/GNSS*, Seoul, Korea, Nov. 2000.

[10] P. Misra and P. Enge, *Global Positioning System signals, Measurements, and Performance*. Lincoln, MA: Ganga-Jumuna Press, 2001.

[11] S. Langel, S. Khanafseh, F. C. Chan, and B. Pervan, "Cycle Ambiguity Reacquisition in UAV Applications Using a Novel GPS/INS Integration Algorithm," *Proceedings of the International Technical Meeting of the Satellite Division of the Institute of Navigation ION-ITM 2009*, Anaheim, CA, Jan. 2009.

[12] R. Brown, "A Baseline RAIM Scheme and a Note on the Equivalence of Three RAIM Methods," *NAVIGATION: Journal of The Institute of Navigation*, vol. 39, No. 3, Fall 1992.

[13] B. Parkinson, and P. Axelrad, "Autonomous GPS Integrity Monitoring Using the Pseudorange Residual," *NAVIGATION: Journal of The Institute of Navigation*, vol. 35, No. 2, 1988.

[14] J. Crassidis and J. Junkins, *Optimal Estimation of Dynamic Systems*. New York, NY: Capman & Hall/CRC, 2004.

[15] S. Khanafseh, B. Kempny, and B. Pervan, "New Applications of Measurement Redundancy in High Performance Relative Navigation Systems for Aviation," *Proceedings of the 19th International Technical Meeting of the Satellite Division of the Institute of Navigation ION GNSS 2006*, Fort Worth, TX, Sept. 2006.

[16] G. A. McGraw "Generalized Divergence-Free Carrier Smoothing with Applications to Dual Frequency Differential GPS," *NAVIGATION: Journal of Institute of Navigation,* vol. 56, No. 2, Summer 2009.

[17] P. Teunissen, "GNSS Ambiguity Bootstrapping: Theory and Application," *Proceeding KIS2001, International Symposium on Kinematic Systems in Geodesy, Geomatics and Navigation*, Bnaff, Canada, 2001.

[18] S. Khanafseh and B. Pervan, "A New Approach for Calculating Position Domain Integrity Risk for Cycle Resolution in Carrier Phase Navigation Systems," *Proceeding of the IEEE/ION Position, Location, and Navigation Symposium (PLANS '2008)*, Monterey, CA, Apr. 2008.

[19] D. Chiu and K. O'Keefe, "Bierman-Thornton UD Filtering for Double-Differenced Carrier Phase Estimation Accounting for Full Mathematical Correlation," *Proceedings of the Institute of Navigation 2008 NTM Meeting*, San Diego, CA, Jan. 2008.

[20] A. Bryson, *Applied Linear Optimal Control: Examples and Algorithms* New York, NY: Cambridge University Press 2002.

[21] K. O'Keefe, M. Petovello, G. Lachapelle, and M. Cannon, "Assessing Probability of Correct Ambiguity Resolution in the Presence of Time-Correlated Errors," *NAVIGATION: Journal of Institute of Navigation,* vol. 53, No. 4, Winter 2006.